

Core surface flow modelling from high-resolution secular variation

R. Holme¹ and N. Olsen²

¹Department of Earth and Ocean Sciences, University of Liverpool, UK. E-mail: holme@liv.ac.uk

²Danish National Space Center, Copenhagen, Denmark

Accepted 2006 April 4. Received 2006 January 9; in original form 2004 September 3

SUMMARY

Data from the Ørsted and CHAMP satellites have allowed modelling of the geomagnetic secular variation (SV) with unprecedented accuracy. The spectrum of the SV is consistent with generation by advectively dominated processes. Based on the SV model, it is not possible to reject the frozen-flux hypothesis, but the spectrum of the SV implies that a conclusive test of frozen-flux is not possible. We parametrize the effects of diffusion as an expected misfit in the flow prediction due to departure from the frozen-flux hypothesis; at low spherical harmonic degrees, this contribution dominates the expected departure of the SV predictions from flow to the observed SV , while at high degrees the SV model uncertainty is dominant. We construct fine-scale core surface flows to model the SV . Flow non-uniqueness is a serious problem because the flows are sufficiently small scale to allow flow around non-uniqueness contours. Nevertheless, we find evidence to support previously suggested polar vortices. For this model of field and SV , predicted variations in length of day from modelled core angular momentum vary over a large range, although there is evidence that this effect is reduced with longer time-series of magnetic data and better parametrization of the external magnetic field.

Key words: core flow modelling, geomagnetic secular variation, length-of-day variation.

1 INTRODUCTION

The geomagnetic field is a sensitive probe of the structure and dynamics of the Earth, particularly the deep Earth. It shows significant variations down to decadal timescales and shorter, much shorter than most processes involving the Earth's interior geodynamics. These changes, named magnetic secular variation (SV), have been used to study core–mantle interactions, and to constrain flow in the core and the dynamo process responsible for generating the field. However, the scope of such studies has been restricted by limitations in the data used to determine models of the SV . Magnetic observatories provide high-quality time-series of measurements, in some cases exceeding 100 yr, but their distribution over the Earth's surface is too sparse and uneven to enable full advantage to be taken of the quality of data. Satellite measurements can provide global coverage, but low-Earth orbit, three-component, vector data are necessary to obtain accurate field models. Until recently, only the Magsat satellite had provided such data, but it flew for less than a year (in 1979–1980). While the data provided enabled the production of detailed global models of the field at that epoch (e.g. Cain *et al.* 1989a), the mission lifetime was too short to model accurately the changes in the field, and, in particular, to separate these changes from short (yearly and less) period variations resulting from magnetic fields external to the Earth.

However, two recent satellite missions have improved this position enormously. Ørsted, launched in 1999 February (Neubert *et al.* 2001), and CHAMP, launched in 2000 July (Reigber *et al.* 2002), are both polar, low-Earth orbiting satellites, and have pro-

vided broadly continuous globally distributed vector magnetic measurements since their launch. These data have yielded very accurate models of the magnetic field (e.g. Olsen *et al.* 2000; Olsen 2002; Maus *et al.* 2002; Sabaka *et al.* 2004). Hulot *et al.* (2002) have considered what the difference in the field between 1980 and 2000 can tell us about core processes. However, additionally, sufficient data are now available to provide good models of the SV over the period of the satellite missions.

In this paper, we examine one such model, the CO2003 model, determined from satellite data covering the period 1999 March to 2003 July. The modelling methodology is described by Olsen (2002), with more specific details of model construction, such as parametrization of external fields, given by Holme & Olsen (2005). We begin by summarizing key features of the process by which we model the flow at the core–mantle boundary (CMB) from magnetic SV . We examine the CO2003 model in detail, focusing on properties of its spatial spectrum, and testing it against a measure of frozen-flux. We develop a parametrization for treating the effects of diffusion as an error on the use of observed SV to model core surface flow, and with this parametrization generate detailed models of the flow at the CMB. Finally, we use variation in flow over the period of the satellite missions to compare predictions of variation in core angular momentum (CAM) with observed length of day (LOD).

2 CORE FLOW MODELLING

We summarize here some aspects of surface core flow modelling from SV . Reviews of this procedure are given by Bloxham & Jackson

(1991) and Whaler & Davis (1997). Secular variation from the core arises from two processes, advection of the field by the flow, and field diffusion. For the radial component of the field B_r at the CMB, we may write

$$\dot{B}_r + \nabla_H \cdot (\mathbf{u}B_r) = \frac{\eta}{r} \nabla^2(rB_r), \quad (1)$$

where \mathbf{u} is the core surface flow, r the radial coordinate, η is magnetic diffusivity, and the dot denotes a time derivative. The horizontal divergence $\nabla_H \cdot (\mathbf{u}B_r)$ describes advection of the field by the flow, while $\frac{\eta}{r} \nabla^2(rB_r)$ describes diffusion. Direct calculation of the diffusion term in the region of the flow (the top of the free stream) is not possible from observations. However, a simple scaling analysis of each term, assuming length scale L and velocity scale U gives the ratio of the advective term to the diffusive term as the magnetic Reynolds number: $R_m = UL/\eta$. Typical scales in the core might be $U \simeq 5 \times 10^{-4} \text{ m s}^{-1}$, $L \simeq 1000 \text{ km}$, $\eta \simeq 1 \text{ m}^2 \text{ s}^{-1}$ giving $R_m \approx 500$, suggesting that advection dominates diffusion. (Many weaknesses in this argument are discussed by Bloxham & Jackson (1991).) If diffusion is neglected, then the so-called frozen-flux theorem applies: the magnetic field is frozen into the fluid, and so acts as a tracer for core flow. This assumption underlies most studies of core surface flow, especially for models of time-dependent flow (see Voorhies 1993, for steady flows determined including a parametrization of diffusion).

Even ignoring diffusion, flow inversion is *non-unique*. This non-uniqueness was first formally phrased by Backus (1968), but can be understood more simply, in that a single equation

$$\dot{B}_r + \nabla_H \cdot (\mathbf{u}B_r) = 0 \quad (2)$$

(eq. 1 leaving out the diffusion terms) is used to determine two components of flow (for example the northwards and westwards component—the vertical component is assumed to be zero from an impenetrable spherical CMB). To construct flow models constrained by SV , further assumptions are necessary as to the nature of the flow. The most fundamental is that the flow is large scale: this is commonly implemented through regularization (damping). To make additional progress, flows have been calculated constrained with additional assumptions concerning their dynamics. The simplest such assumption has been to assume that the flow is steady in time (Gubbins 1982; Voorhies & Backus 1985), recently extended to consider the flow steady in a drifting frame (Holme & Whaler 2001). However, two other assumptions have more generally been adopted: firstly, that the flow is toroidal (minimal upwelling at the CMB, motivated by suggestions that the top of the core may be stably stratified) (Whaler 1980), and secondly, that the flow is tangentially geostrophic (only weak non-radial gravity or Lorentz force at the CMB, giving a first-order horizontal force balance between pressure gradients and Coriolis force) (Hills 1979; Le Mouél 1984). Note that it is not possible to explain the secular variation through fluid flow if both of these assumptions hold (Bloxham 1990). Perhaps surprisingly, whichever assumption has been adopted (steady, toroidal or tangentially geostrophic), the flows calculated have looked broadly similar (Bloxham & Jackson 1991).

For both the toroidal and geostrophic approximations, the non-uniqueness can be understood quite simply. Toroidal incompressible flow implies $\nabla_H \cdot \mathbf{u} = 0$, which substituted into eq. (2) yields

$$\dot{B}_r + \mathbf{u} \cdot \nabla_H B_r = 0. \quad (3)$$

Allowing for continuity conditions, the flow is undetermined along contours of B_r , both around local maxima and minima in the field, but also along the magnetic equator. Similarly, tangentially

geostrophic flow satisfies $\nabla_H \cdot (\mathbf{u} \cos \theta) = 0$, where θ is colatitude, which substituted into eq. (2), yields

$$\dot{B}_r + \cos \theta \mathbf{u} \cdot \nabla_H (B_r / \cos \theta) = 0. \quad (4)$$

In this case, flow is undetermined along closed contours of $B_r / \cos \theta$. The geostrophic assumption is more powerful than the toroidal one, because any geostrophic contour that crosses the equator does not imply non-uniqueness (Backus & Le Mouél 1986). As a result, the flow is formally non-unique only in patches of the core surface, called ambiguous patches. This seems encouraging, but unfortunately dynamo models suggest strong flows along just such contours (Rau *et al.* 2000).

Given this non-uniqueness, not to mention the neglect of diffusion, how can we assess further whether modelled surface core flows are in any way related to the true flow? The one piece of corroboratory evidence comes from comparison with observations of decadal variation in LOD. For over half a century, it has been postulated that such decadal variations arise from exchange of angular momentum between the fluid core and the solid mantle (see, e.g. Vestine 1953). Braginsky (1970) argued that flow in the core which supported such variations would be uniform on cylinders, co-axial with the rotation axis. Jault *et al.* (1988) made the crucial observation that if this were the case, changes in models of core surface flow could reflect changes deep within the core, and allow calculation of the overall change in CAM. The most convincing demonstration of this is that of Jackson *et al.* (1993), who found a good correlation between observed variations in LOD and the predicted changes in CAM, at least for the twentieth century. Note, however, that this constraint only concerns changes in one part of the flow: the steady part of the flow does not affect Earth rotation, and so is not corroborated by this independent observation.

3 A PARAMETRIZED MODEL OF THE SECULAR VARIATION

The magnetic field \mathbf{B} originating from within the Earth measured at the Earth's surface can be represented as the gradient of a scalar potential Φ satisfying Laplace's equation, so that $\mathbf{B} = -\nabla\Phi$ and $\nabla^2\Phi = 0$. In spherical geometry, the solution to this eq. can most conveniently be expressed in terms of spherical harmonics

$$\Phi = a \sum_{l=1}^{\infty} \left(\frac{a}{r}\right)^{l+1} \sum_{m=0}^l P_l^m(\cos \theta) (g_l^m \cos m\phi + h_l^m \sin m\phi). \quad (5)$$

Here, (r, θ, ϕ) are spherical coordinates given by distance from the centre of the Earth, colatitude and longitude, a is the radius of the Earth (taken as 6371.2 km), and P_l^m are Schmidt semi-normalized associated Legendre functions in $\cos \theta$, of degree l and order m . $\{g_l^m, h_l^m\}$ are the set of Gauss coefficients which parametrize the field, determined in the CO2003 model with quadratic time dependency

$$\begin{aligned} g_l^m &= g_l^m|_{t=t_0} + \dot{g}_l^m|_{t=t_0}(t-t_0) + \frac{1}{2}\ddot{g}_l^m|_{t=t_0}(t-t_0)^2 \\ h_l^m &= h_l^m|_{t=t_0} + \dot{h}_l^m|_{t=t_0}(t-t_0) + \frac{1}{2}\ddot{h}_l^m|_{t=t_0}(t-t_0)^2 \end{aligned} \quad (6)$$

where $t_0 = 2001.0$, and the series of Gauss coefficients is truncated at harmonic degree $l = 40$ for the constant terms, $l = 16$ for the secular variation terms, and $l = 8$ for the secular acceleration terms. Thus, at time t , the coefficients of the secular variation are given by

$$\begin{aligned} \dot{g}_l^m &= \dot{g}_l^m|_{t=t_0} + \ddot{g}_l^m|_{t=t_0}(t-t_0) \\ \dot{h}_l^m &= \dot{h}_l^m|_{t=t_0} + \ddot{h}_l^m|_{t=t_0}(t-t_0) \end{aligned} \quad (7)$$

We begin by examining the spectrum of the secular variation, a methodology which has previously proved fruitful for studying the geomagnetic field. Various authors (e.g. Mauersberger 1956; Lowes 1974) noticed independently that the mean-square value of the field, integrated over a spherical surface, has a simple form

$$\frac{1}{A} \oint \mathbf{B} \cdot \mathbf{B} dA = \sum_{l=1}^{\infty} (l+1) \left(\frac{a}{r}\right)^{2l+4} \sum_{m=0}^l \left((g_l^m)^2 + (h_l^m)^2 \right), \quad (8)$$

where A is the area of the sphere at radius r . It is then instructive for a given radius r to plot the individual contributions to this integral from components of different degree l (effectively wavenumber) against that degree, giving a “power spectrum” of the field. This form of the spectrum is most commonly referred to as the Lowes spectrum, and it has been used, amongst other things, to justify a separation between source contributions from the Earth’s core and lithosphere (Langel & Estes 1982), to provide a geomagnetic estimate of the depth to the CMB (Voorhies *et al.* 2002; Voorhies 2004), and as a tool for examining errors in magnetic models (Cain *et al.* 1989b; Holme & Jackson 1997). Here, we consider a similar spectrum for the mean-square secular variation, plotting

$$(l+1) \left(\frac{a}{r}\right)^{2l+4} \sum_{m=0}^l \left((g_l^m)^2 + (h_l^m)^2 \right), \quad (9)$$

against l . In Fig. 1 this spectrum is plotted for three different field models, calculated at the Earth’s surface $r = a$. ufm (Bloxham & Jackson 1992) is representative of the resolution of the SV prior to Ørsted and CHAMP, constrained by data from the Magsat satellite and magnetic observatories. Two models are presented from Holme & Olsen (2005), the first obtained only by a least-squares fit to data, and the second (the CO2003 model) with additional weak regularization to minimize the SV power at the CMB. At low harmonic degree, all spectra fit closely an exponential behaviour (a straight line on this linear-logarithmic plot). The ufm model deviates from power law behaviour above harmonic degree $l \approx 7$. This is the point at which model regularization (damping) becomes dominant in the model: in other words, the data were insufficient to constrain secular variation above this degree. CO2003 maintains exponential behaviour to degree 12. The behaviour of the undamped model at higher degree is symptomatic of the effects of random errors in the data; the weak damping of the CO2003 model constrains the spectrum to fall off at degree 13 and above.

Of physically more interest is the SV spectrum at the CMB ($r = c$), where we believe the magnetic field to originate, plotted in Fig. 2. Again ufm (1980) falls off above degree 7, while the spectrum of the new undamped model rises rapidly above degree 12, again con-

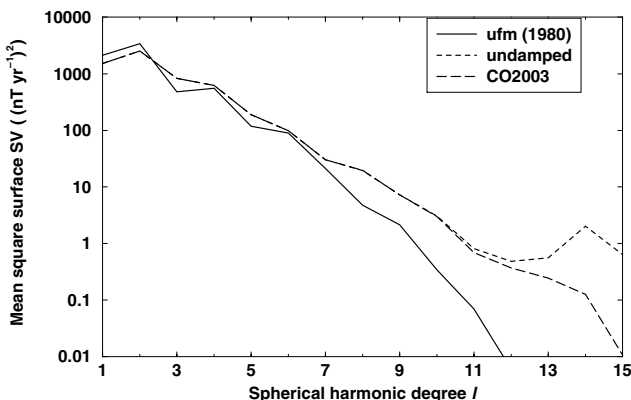


Figure 1. Spectra of SV models at Earth’s surface.

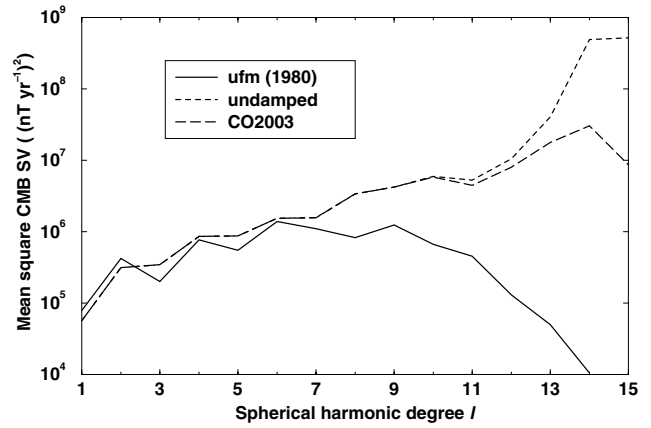


Figure 2. Spectra of SV models at CMB, $r = c$.

sistent with sources of error dominating the spectrum at these wavelengths. Plotting at $r = c$ emphasizes additional interesting details, for example “steps” in the spectra: each spectrum shows a sharp increase from $l = \text{odd}$ to $l = \text{even}$, and is flat or decreases from $l = \text{even}$ to $l = \text{odd}$. Most obviously, however, the spectra are ‘blue’—their power increases with degree. A simple interpretation based on ‘white noise’ sources would suggest a SV source depth above the CMB—the prediction from the CO2003 model is a depth of $0.66a$ (in middle of lower mantle). There is no known source for SV at this depth.

The spectrum (eq. 9) we have considered is convenient, but many other more physically motivated spectra are possible, with different functions of l as prefactors; see Voorhies (2004) for detailed discussion plus extensive references. To avoid a somewhat arbitrary choice of spectrum, following McLeod (1985, 1996), we consider the degree by degree ratio of the power in the SV to that in the main field, plotting

$$R(l) = \frac{\sum_{m=0}^l \left((g_l^m)^2 + (h_l^m)^2 \right)}{\sum_{m=0}^l \left((g_l^m)^2 + (h_l^m)^2 \right)}, \quad (10)$$

against l . This function is independent of both definition of spectrum (the dependence on l in the prefactor cancels in the ratio), and of depth r . Degrees 1 and 2 are known to be anomalous in both the main field power spectrum and the SV spectrum (Voorhies 2004), while degree 13–14 are affected by errors in SV , and controlled by regularization, and by lithospheric field contribution to the main field. We fit the remaining degrees ($l = 3$ –12) with two different functions. First, we fit an exponential curve $R = Ae^{Bl}$, which would be consistent with fitting a different source depth for the main field and SV ; the source depth ratio would be $\exp(B/2)$. Secondly, we fit a power law $R = Al^B$, which would be consistent with a different spectral definition for the main field and SV . These fits are presented in Fig. 3. The power law curve fits the model better than the exponential curve, and the residuals show less of a trend with degree. In addition, the dipole term ($l = 1$) is better predicted, and the fit to degrees 13 and 14 is consistent with the applied regularization. The exponent of this curve is $B = 2.9$. We conclude that there is no reason to assume a different source depth for the SV and main field, but instead their spectra take different forms.

Why should this be? A different spectral form for field and SV has been proposed before: McLeod (1996) predicted a ratio $\sim l^4$ (i.e. $B = 4$) (see also Voorhies 2004). The ratio has also been discussed in terms of the characteristic timescale of variation of the field at a

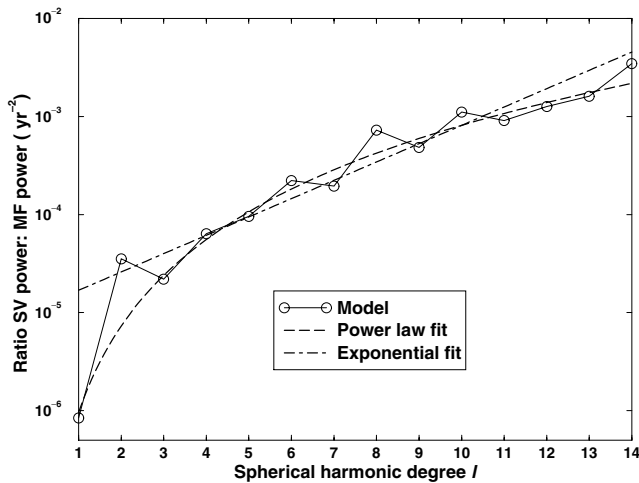


Figure 3. Fit to ratio of spectral power in *SV* and main field. Exponent for power law fit is $B = 2.9$.

given wavenumber (Hulot & Le Mouél 1994; De Santis *et al.* 2003). (The results of De Santis *et al.* (2003) are equivalent to $B = 3.2$ in our treatment.) Our fit yields a characteristic timescale in years of

$$\tau \approx 1000l^{-1.45}, \quad (11)$$

giving approximately 20 yr for $l = 14$. We appeal to a simpler interpretation. The relation for generation of *SV* is given in eq. (1). If horizontal and radial length scales are similar then scaling analysis would suggest that for diffusion $\nabla^2 \sim l(l+1)$ leading to $R \sim l^4$, while for advection $\nabla_H \sim l$, suggesting $R \sim l^2 f(l)$ where $f(l)$ would be an unknown complicated function depending on field/flow interactions, and in particular the evaluation of Gaunt and Elsasser integrals (e.g. Whaler 1986). Despite this uncertainty, a power law relation for R between l^2 and l^4 seems plausible. The uniformity of the power law also suggests a related balance of advective and diffusive processes at all degrees. Thus, if it is sensible to model core surface flow from low-degree *SV*, there seems no reason to preclude modelling flow from the new, higher resolution, *SV*.

We caution at this stage against detailed interpretation of the exponent $B = 2.9$. We note that a preliminary version of CO2003, from only slightly fewer data than the model used here, predicted an exponent of $B = 3.4$. Thus, the value of this coefficient appears uncertain. More detailed analysis should await detailed field models from longer data series.

4 A TEST OF THE FROZEN-FLUX APPROXIMATION

Modelling of flow with conventional methods relies on the frozen-flux approximation. From this assumption follow certain predictions about the evolution of the field which may be tested for magnetic models (see, for example, Jackson & Hide 1996). For example, the hypothesis predicts that null-flux curves (lines of $B_r = 0$ at the CMB) can be neither created nor destroyed. As even very weak diffusion would allow this condition to be violated, we instead apply a less sensitive test. The total unsigned flux through the CMB is defined

$$\int_{\text{CMB}} |B_r| dA. \quad (12)$$

A necessary (but not sufficient) condition for frozen flux to apply is that this quantity should not change with time (Bondi & Gold

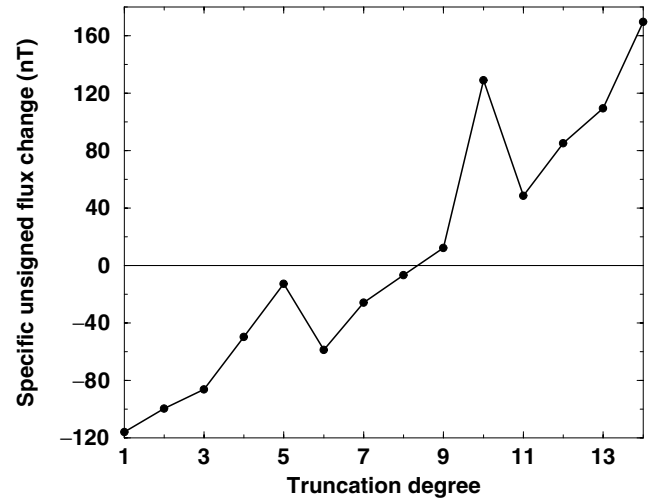


Figure 4. Change in specific integrated unsigned flux between epoch 2000.5 and 2001.5 as a function of model truncation. For example, at degree 7, B_r is calculated at both epochs with Gauss coefficients only up to and including $l = 7$.

1950). It is thus appropriate to test this condition for CO2003 before attempting to model core flow.

We test the CO2003 model against this hypothesis by calculating the difference in this integral between epochs 2000.5, and 2001.5. In Fig. 4, these results are plotted for the model truncated at increasing degree. We choose to plot the results in terms of specific unsigned flux (unsigned flux per unit area of the CMB—or equivalently the mean value of $|B_r|$ at the CMB). The closest fit to frozen flux comes at degrees 7–9, approximately the resolution of pre-Ørsted/CHAMP models, and in agreement with earlier work of Voorhies & Benton (1982). To quantify how close the model at degree 9 is to frozen flux, we combine the CO2003 main field model with randomly generated *SV* coefficients zero mean with variance to match the observed *SV* power spectrum. Of the random models, only 2 per cent generate a smaller change in the specific unsigned flux integral than the model calculated from observations. While this appears to support the idea that CO2003 obeys frozen flux, we recognize that we have chosen the truncation degree which gives the most favourable result.

However, at higher degree, the higher resolution of the CO2003 model appears to lead to a departure from frozen flux. How well constrained is this result? Errors in both the field and *SV* models may compromise the calculation at higher degree. The modelled internal field includes a contribution from the lithosphere, which will be present at all degrees, but of particular significance relative to the main field at degrees 13–14. This field will influence the calculation of the unsigned flux through changing the location of the null-flux curves. Further displacement of the curves would be expected from higher degree field ($l \geq 15$) that is unknown due to screening by the lithosphere. Probably more importantly, the *SV* model cannot be sufficiently well constrained. To examine this problem, keeping the main field and secular acceleration coefficients fixed, we allow small perturbations to the *SV* coefficients. We find a model with a difference in specific unsigned flux of less than 0.1 nT, zero to within the margin of accuracy of numerical integration. In Fig. 5 the *SV* spectrum of the perturbed model is compared with the CO2003 model. The difference between the spectra is well below observational error (Lowes & Olsen 2004), even without considering uncertainties in the main field model.

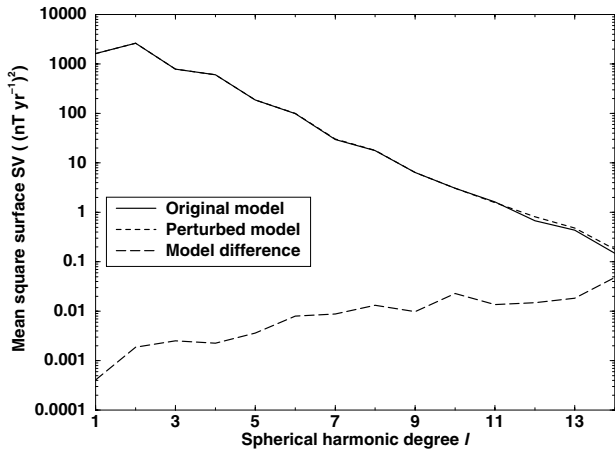


Figure 5. SV spectra for CO2003, a model with slight perturbation which gives no change in the specific unsigned flux integral, and their difference. The difference between the two models is well below observational error.

In conclusion, there is insufficient evidence to reject the hypothesis that the CO2003 model satisfies frozen flux. Note that we do not claim that CO2003 confirms the validity of the frozen-flux approximation. A change of 0.01 nT in a single degree 14 SV coefficient, well within model uncertainties, changes the specific unsigned flux integral calculation by 10 nT, a sensitivity that will increase further at higher harmonic degree. Due to the ‘blue’ CMB spectrum of the SV , and crustal screening of the main field, a conclusive test of the frozen-flux hypothesis is likely never to be possible. A corollary of this is that it will be extremely difficult to use observations to constrain magnetic diffusion at the top of the core.

5 ALLOWING FOR DIFFUSION IN CONSTRUCTING FLOW MODELS

Although we have shown that the CO2003 model is consistent with at least one test of the frozen-flux hypothesis, nonetheless, we would expect diffusion to contribute to the SV at the CMB, and hence to affect the modelling of core surface flow. Further, simple scaling arguments suggest this effect should increase at shorter length scales (higher harmonic degree, giving lower magnetic Reynolds number R_m). There are two options for treating diffusion in flow inversions. First, diffusion could be parametrized, as Voorhies (1993) has done for steady flow and steady diffusion, and for which Gubbins (1996) has provided a formalism for considering time dependence. However, this seems unattractive in an already heavily overparametrized problem. Here instead we attempt to estimate the approximate magnitude of diffusion, and apply it as an uncertainty on the prediction of SV from core flow.

A simple quantitative estimate of the effects of diffusion can be obtained by considering free decay. Were the flow in the core to be ‘switched off’, the magnetic field would gradually diffuse away. If the initial field structure were known, the rate at which this happens could be calculated by expanding the field in the core in terms of its free decay modes (Gubbins & Roberts 1987). These modes, spherical harmonics in (θ, ϕ) and spherical Bessel functions in radius, provide a complete basis on which to expand the field. The contribution to the SV from each such mode would be

$$\dot{B}_{r_l}^{mn} \sim B_{r_l}^{mn} \lambda_l^n, \quad (13)$$

where λ_l^n is the decay rate, proportional to the n th zero of the degree l spherical Bessel function, and independent of m . The values of these

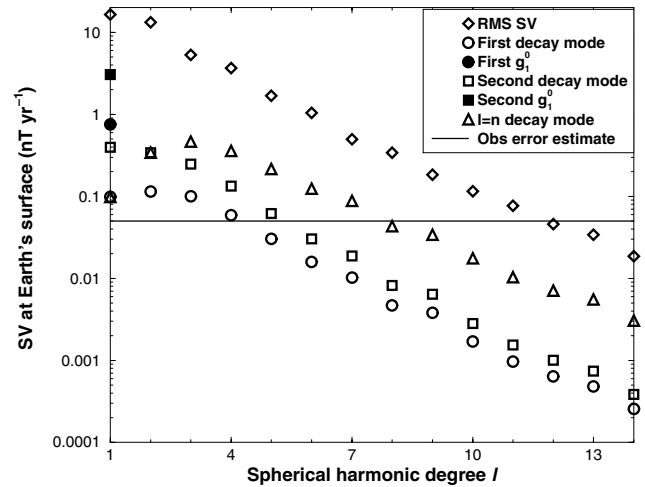


Figure 6. Comparison of SV from free decay modes, observed rms secular variation, and a crude estimate of observational error, plotted at the Earth’s surface. ‘First g_1^0 ’ and ‘Second g_1^0 ’ refer to the SV due to decay of the axial dipole; the other degree 1 terms relate to the equatorial dipole.

zeros are tabulated by Olver (1960). The observed secular variation at the Earth’s surface is then given by upward continuation of this estimate:

$$\dot{B}_{r_l}^m(a) = \dot{B}_{r_l}^m(c) \left(\frac{c}{a} \right)^{l+2}. \quad (14)$$

In Fig. 6, the surface expression of three sets of free decay modes are given, assuming core conductivity of $5 \times 10^5 \text{ S m}^{-1}$ with decay rates based on the first ($n = 1$), second ($n = 2$), and l th ($n = l$) radial mode, where l is the spherical harmonic degree. We take as a characteristic field amplitude the rms contribution to the field at degree l , except for the dipole field, where we treat the axial dipole g_1^0 and the equatorial dipole $\{g_1^1, h_1^1\}$ separately, due to the anomalously large size of the axial dipole. We compare these estimates with CO2003 SV . Fig. 6 also shows pessimistic nominal uncertainties for the secular variation coefficients at 0.05 nT yr^{-1} . The best estimates of the true errors allowing for serial error correlation are more complex (Lowe & Olsen 2004), in particular depending on the harmonic order m , and vary between 0.02 nT yr^{-1} and 0.08 nT yr^{-1} . However, this also does not allow for other sources of secular variation (for example, disturbance due to filtering by a conducting mantle (Benton & Whaler 1983), or oceanic motional induction (Tyler *et al.* 2003)), or for uncertainty due to errors in the main field model (Jackson 1995).

What tentative conclusions may be drawn from Fig. 6? First of all, the observed SV exceeds observational error out to at least degree 11. This, combined with inference from Fig. 1, suggests that our SV model has physical content out to at least this degree. Secondly, because of upward continuation, the magnitudes of the diffusive SV estimates at Earth’s surface fall rapidly with harmonic degree. Thirdly, for each set of free decay modes plotted, the predicted diffusive SV exceeds observational errors at low harmonic degree, but not at higher degree. Thus, perhaps counter-intuitively, it is most important to consider diffusion at *low* harmonic degree, especially for the axial dipole, where the diffusive estimate is particularly high due to the large magnitude of that component of the field. Fourthly, the diffusive estimate approaches the SV only very slowly; on this linear-log plot the curves run approximately parallel to each other. This is particularly clear for the $l = n$ set of modes, for which the decay rates λ_l^n are broadly proportional to l^2 . However, as shown

in Fig. 3, the SV also has a similar power law dependence relative to the field of comparable power ($l^{1.45}$). Hence, considering SV as signal and diffusion as noise, the signal to noise ratio for advective processes may be only weakly dependent on spherical harmonic degree.

We therefore argue that if it makes sense to model flow from low-degree SV , considering only the influence of diffusion, it makes no less sense to extend this procedure to high degree. In fact, from examining Fig. 6, we might suggest that it is most important to consider diffusive effects on SV for the axial dipole field component by approximate increase of the uncertainty for this component. There is some evidence for this from previous flow modelling results; tangentially geostrophic flows often under predict g_1^0 . This can be seen in results of Jackson (1997), and even more clearly with earlier flows from the same author reported by Whaler & Davis (1997). Their Fig. 3 shows that the flow explains well the variation in the axial dipole SV , but its absolute magnitude is under fit by 5–10 nT yr^{-1} , explainable by an unmodelled diffusive component of the secular variation.

What implication does allowing a higher misfit to g_1^0 have compared with previously published flow models? The answer seems to be surprisingly little. Allowing for a higher misfit to the axial dipole term changes the flow pattern very slightly (reducing north-south flow very slightly, making the well-known southern gyre less clear), but the overall pattern remains the same. This is consistent with the flows of Jackson (1997): the axial dipole was already fit anomalously poorly by the flow, so increasing its standard deviation is simply recognizing what the flow models have been trying to tell us.

For the flow modelling in this paper, we adopt a criterion for fit to secular variation coefficients motivated by Fig. 6, calculating a root sum of squares (rss) combination of 0.05 nT yr^{-1} observational error estimate and the diffusive effects based on the $l = n$ mode set (supposing that the radial and lateral length scales might be linked). One exception to this is for the dipole field, because the lowest-order free-decay mode is the slowest possible long-term rate of decay of the field. As the field will have a more complicated structure than this mode, for the dipole field, we take the second free decay mode as our estimate. Overall, diffusive errors are dominant to degree 7, and observational errors at degree 8 and above.

6 MODELLING HIGHER RESOLUTION FLOWS

Encouraged by the arguments of the previous sections, we use the CO2003 SV model to attempt to generate detailed flow images. Hulot *et al.* (2002) have previously attempted similar modelling. However, they estimated the average SV over 20 yr by differencing main field models from 1980 and 2000. 20 yr is only slightly less than the characteristic timescales we have obtained for high-degree SV ; therefore, use of instantaneous estimates of SV will be preferable. We seek a least-squares fit to the SV model, subject to the weighting based on the free-decay modes described above. The flows are expanded in vector spherical harmonics, truncated to harmonic degree 14, as are the expansions for the main field and SV . Technical details of the procedure are given by Whaler (1986). The flows are constrained to be tangentially geostrophic or toroidal by damping (e.g. Holme 1998), and regularized using the so-called ‘strong norm’ of Bloxham (1988). The damping for our new flows was chosen so as to provide a good fit of the SV to harmonic degree 9, as is suggested by the consideration of the unsigned flux integral.

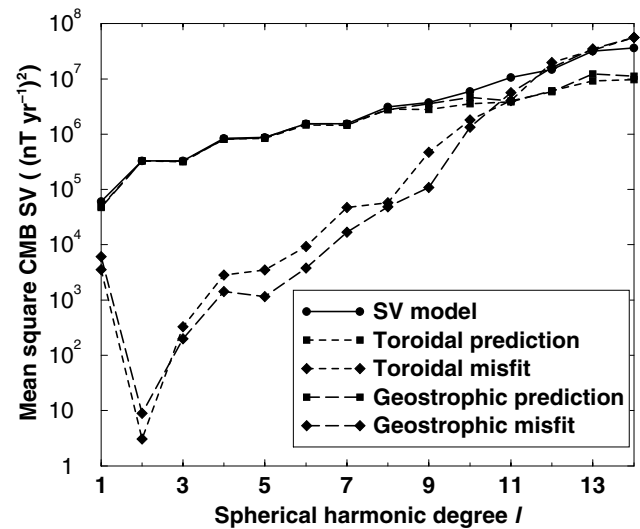


Figure 7. Power spectra predicted by flow models compared with original SV . Note the elevated misfit power spectrum at degree 1, corresponding to the large diffusive uncertainty on the axial dipole SV .

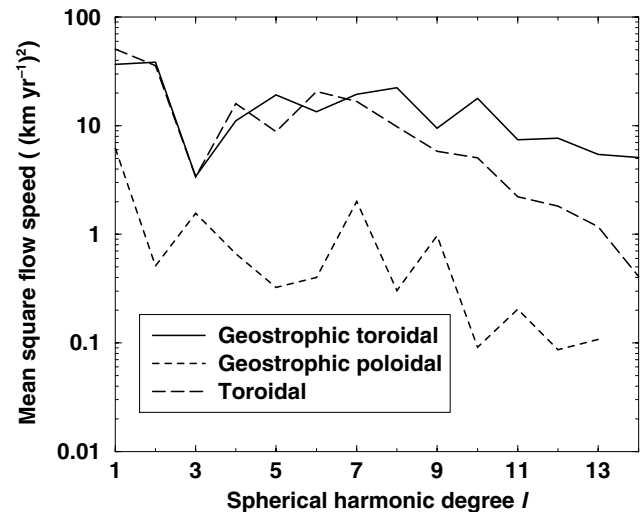


Figure 8. Power spectra for flows. For a geostrophic flow truncated at degrees 13–14, the poloidal power at degree 14 is required to be 0.

Fig. 7 shows the power spectra of the input secular variation model at the CMB, the fits given by our chosen geostrophic and toroidal flows for epoch 2001.0, and the power spectra of their differences. The absolute value of the misfit implied by our parametrization for diffusional error is not strongly motivated: the l^2 dependence of the diffusional SV at the CMB arising from the free decay modes seems plausible, but the scaling prefactor governing the overall strength of diffusion is unknown. Instead of fitting closely to one standard deviation, we try to fit the general properties of the SV .

Both flows show much more small scale structure than most previously published flows. A plot of the power spectra of the two flows (in Fig. 8) shows that, while neither flow is truly ‘converged’ in the sense that their power at high degree is minimal, nevertheless that power decreases with degree above degree 7. Despite this decrease, the flows are still able to generate the ‘blue’ spectrum of SV at the CMB; as discussed earlier, advection will naturally produce at least a spectral dependence $\sim l$, so reaching $\sim l^{1.45}$ is not especially difficult.

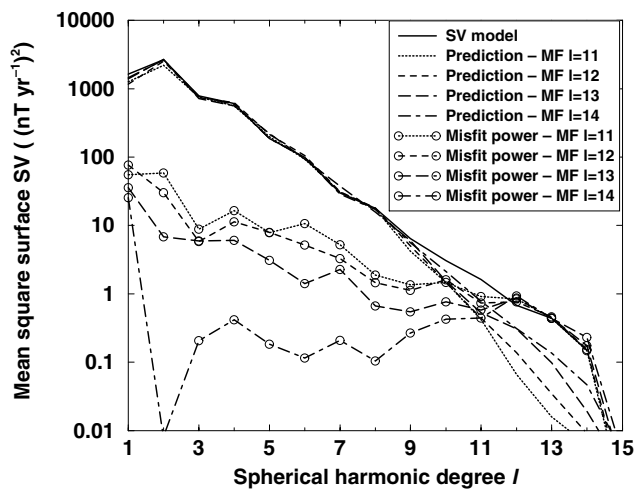


Figure 9. Power spectra of flow model predictions and differences from the input model for main field truncated to degrees $l = 11, 12, 13, 14$.

As noted above, the main field at degree 14 is of uncertain origin, and a significant part may originate from lithospheric rather than core sources. In Fig. 9 we examine the influence of the high-degree main field by considering the predicted secular variation of the geostrophic flow with main field model truncated to degrees $l = 11, 12, 13, 14$. Clearly, the SV is less well fit, but the changes are still small compared with the power of the SV . We therefore conclude that our flow models are not highly sensitive to high-degree main field errors. (Note that this conclusion is in contrast with that of Eymin & Hulot (2005), who identify unknown high-degree main field as a primary source of error in flow modelling.)

We plot in Fig. 10 the geostrophic flow and the toroidal flow, together with their contours of non-uniqueness as defined from eqs (3) and (4). Both flows show strong equatorial symmetry, and much small-scale structure. Individually, these flows do not show strong signs of non-uniqueness when compared with the non-uniqueness contours. However, detailed features vary with the *a priori* information: for example, an eastward flow under central Asia leading to a vortex there in the geostrophic flow is absent in the toroidal flow. Some features are common to both flows: for example, small vortices below Siberia and the southern Indian ocean which also do not overlie areas of non-uniqueness, and so may be robust. Note also that these features are at approximately the same longitude, but antisymmetric with respect to each other. It could be that the vortices are the ends of a column of fluid convection, perhaps similar to the thin rotating columns of fluid often referred to as Busse rolls (e.g. Roberts 1987). There are slight indications of similar features at about 20 and 90 W. We have generated flows that show this pattern more clearly, but also flows that show no such feature, so we choose to present the ambiguous case and suggest further study may be rewarding.

How do our results compare with those of Hulot *et al.* (2002)? These authors produced fine-scale flows by differencing Magsat and Ørsted models of the field in 1980 and 2000 respectively. The large-scale flow structure is not dissimilar, but the small-scale structure differs considerably. This might arise from their different method of estimating SV . However, significantly, their flows include many small vortices in mid latitudes, which coincide with contours of the geostrophic degeneracy. The minimum norm approach used here tries to minimize a measure related to flow intensity, and so will suppress the vortices unless their presence reduces the overall flow

strength. These or similar vortices may nevertheless be a feature of the true flow: circulation around closed field contours is a feature of some numerical dynamo models (Olson *et al.* 1999). Nevertheless, much of the small-scale structure of the Hulot *et al.* (2002) model, while not in conflict with the data, is not required by it. (More recent models of Eymin & Hulot (2005) do not show these vortices so strongly.)

Non-uniqueness now can be clearly seen in some flows, whereas formally different flow types all looked similar. Why is this? Looking at the contour plots of non-uniqueness (Figs 10c and d) it is clear, particularly for the tangentially geostrophic case, that to construct a flow along such contours requires detailed flow structure. Previously, flows were sought with such small-scale detail eliminated by damping. As a result, formal non-uniqueness was comparatively unimportant, and so flow structure, controlled by the SV and the large-scale assumption, was similar whatever the additional *a priori* information. Constructing more detailed flows as here, this is no longer the case. To summarize, new fine-scale flows show more variation with *a priori* information, and more variation between different studies. Thus, detailed interpretation of flow structure should proceed with extreme caution.

Our flows do show evidence of a larger structure reported by Hulot *et al.* (2002): polar vortices at both the North and South Poles. A polar vortex for the North Pole was first proposed by Olson & Aurnou (1999) from local area flow modelling from the ufm field model of Bloxham & Jackson (1992). Hulot *et al.* (2002) confirmed this feature, and also suggested the presence of a vortex around the South Pole in the same sense. To investigate this feature in our flows, we plot in Fig. 11 the axial angular velocity for the tangentially geostrophic and toroidal flows shown above. Both models have vortices at both poles. The symmetry reported by Hulot *et al.* (2002) is not seen in the geostrophic model, perhaps due to the use of point estimates for secular variation rather than temporal averages, giving noisier results. However, it is more probable that again the difference results from different methodology in dealing with flow non-uniqueness. There is also a non-unique patch encompassing the North Pole in both the toroidal, and particularly the geostrophic, non-uniqueness, as shown in Fig. 12: this means that the flow model can be constructed with considerable ambiguity in the net circulation about this point. The original observation of the vortices by Olson & Aurnou (1999) focused on the movement with time of the field contours, their flow was zonal, and so did not allow for an arbitrary flow along these contours (or close to them).

Even with the polar vortices, one serious problem of interpretation remains, alluded to by Voorhies (1993), identified by Gubbins & Kelly (1996), and revisited by Love (1999). If the flow is steady, or slowly varying, as is often suggested, then the magnetic field evolves to an equilibrium between advective and diffusive processes. Then the primary balance in eq. (1) is between advection and diffusion, rather than advection and SV . As a result, the SV is given by the imbalance between two closely balanced processes, rather than only the flow. Rau *et al.* (2000) examined the role of advection and diffusion in a dynamo simulation, and found this balance to be present, but nonetheless that the flow could be recovered from SV quite well (although they suggested that the limited spatial resolution of geomagnetic models might pose more of a problem).

7 ANGULAR MOMENTUM

As mentioned in Section 2, agreement between estimated CAM and observed LOD variation provides some support for flow modelling.

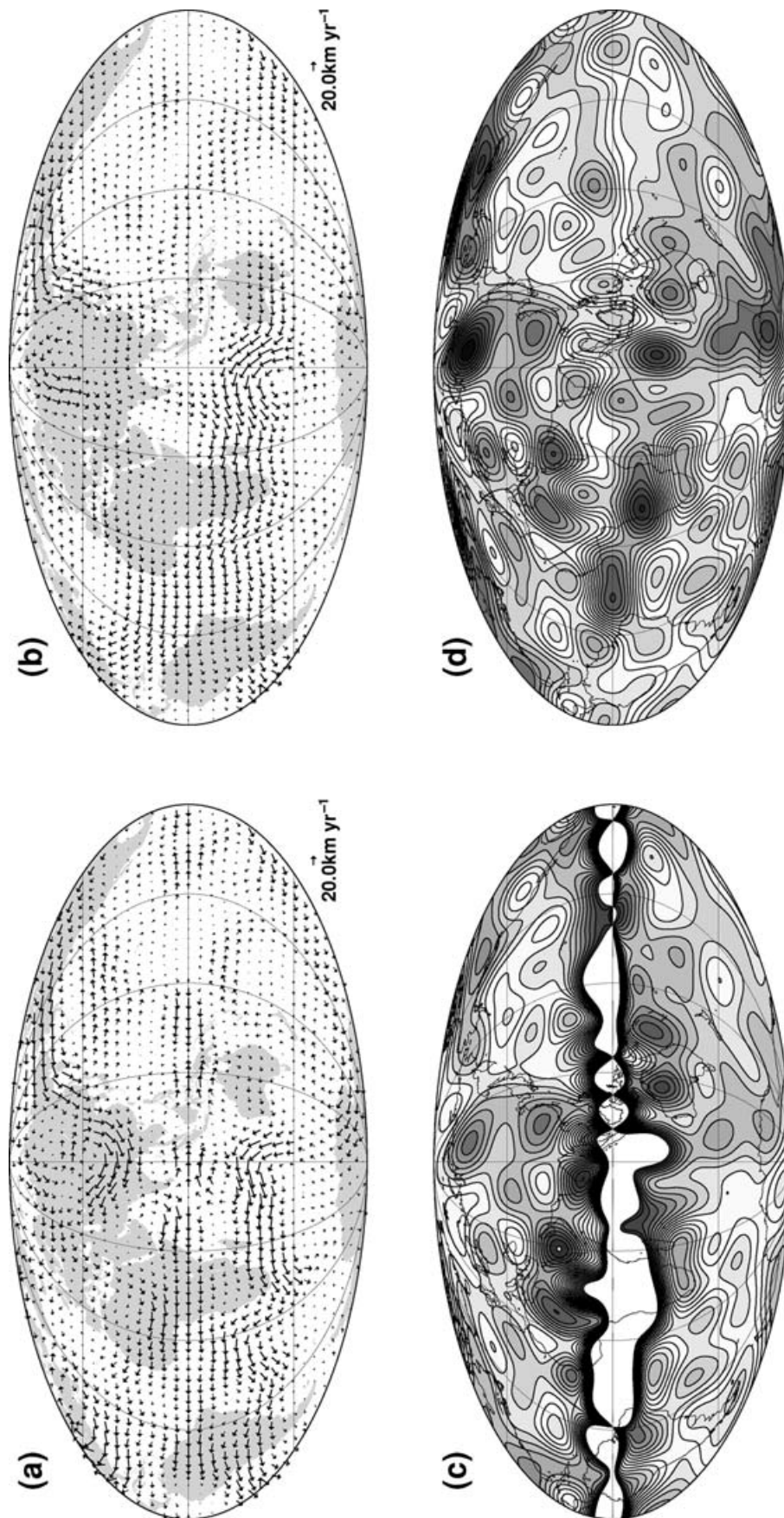


Figure 10. (a) Geostrophic flow model. (b) Toroidal flow model. Continents included to provide a reference frame. (c) Geostrophic non-uniqueness contours. (d) Toroidal non-uniqueness contours. Flow along closed contours in (c), and all contours in (d) would generate no secular variation, and so is not detectable from geomagnetic observations. In both (c) and (d), shading scale not relevant, but included to emphasize areas of local maximum/minimum.

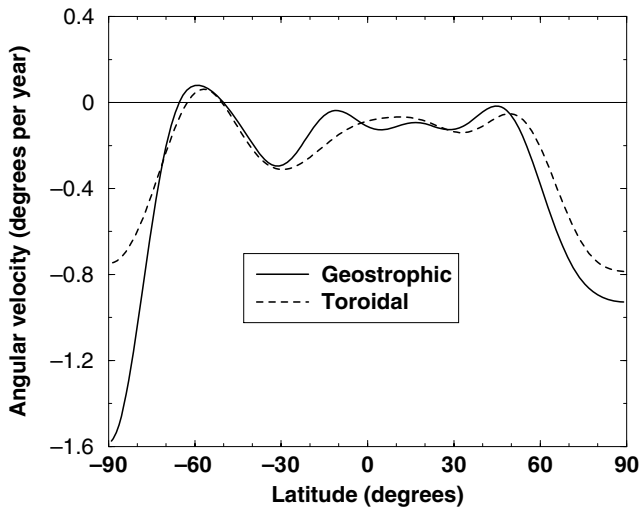


Figure 11. Axial toroidal velocity component as a function of latitude, suggesting polar vortices.

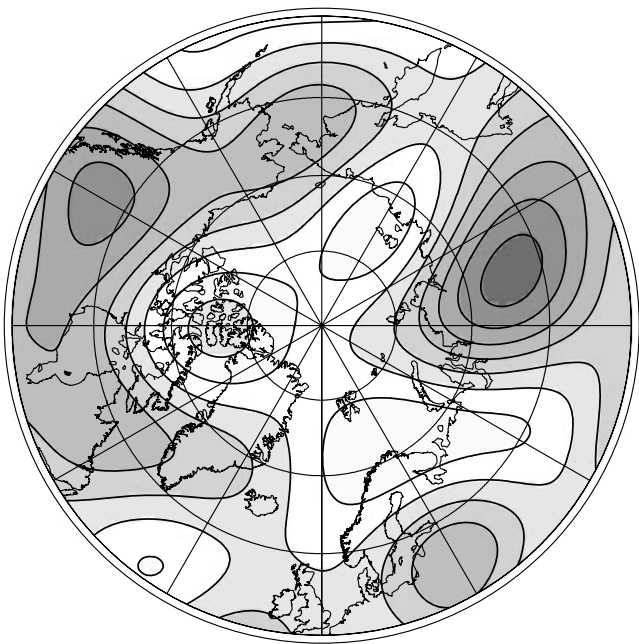


Figure 12. Non-uniqueness contours for geostrophic flows near the North Pole.

It is therefore of great interest to examine the changes in the fine-scale flows we have calculated over the period of the CO2003 model, and compare the predicted CAM variation with observed LOD variations. The absolute angular momentum of the core cannot be calculated from the flows, but an estimate of change in CAM is given by a simple formula (Jackson *et al.* 1993), depending on changes in only two zonally symmetric toroidal flow harmonics. In Fig. 13 we plot the angular momentum predicted from flow modelled at yearly epochs from 1999.5 to 2003.5 for a set of flows of increasing complexity, as demonstrated by the fit to nominal σ given in the legend. We compare these predictions with the decadal LOD curve of Holme & de Viron (2005), who provide a clean time-series for decadal Δ LOD by subtracting from the observations a model of atmospheric angular momentum, and taking a one-year running av-

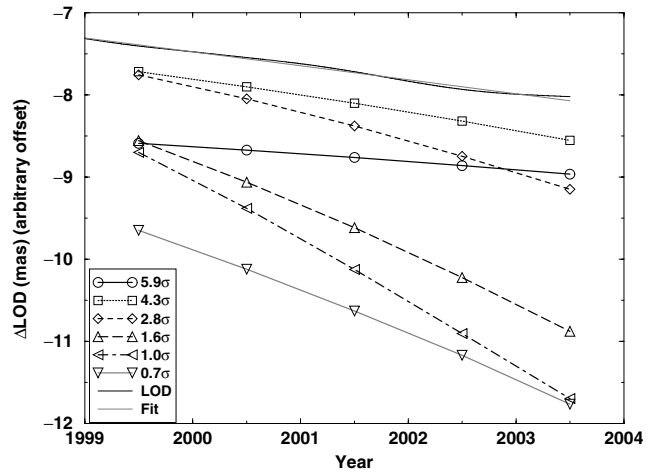


Figure 13. Angular momentum calculation for single epoch flows, compared with shifted observed length-of-day (LOD) variation and a straight line fit to this. The offset between the various curves is arbitrary, and can be shifted up and down.

erage to remove unmodelled annual, semi-annual and terannual signal from unmodelled atmospheric and oceanic angular momentum. Between 1999.5 and 2003.5, the rate of decrease of LOD is almost constant at 0.170 ms yr^{-1} . Tidal forces cause a secular increase in LOD, generally assumed to be about 0.014 ms yr^{-1} (Stephenson & Morrison 1995). Thus, the rate of change in LOD over the period which could arise from core–mantle angular momentum exchange is a decrease in LOD of 0.184 ms yr^{-1} .

As can be seen, the different flows give a wide range of predicted LOD variation, between -0.10 ms yr^{-1} and -0.76 ms yr^{-1} . A straight-line fit to each data set yields the rate of change of CAM, and also motivates modelling SV with flows with constant acceleration (Voorhies 1995). Such flows are fully consistent with a geomagnetic field that is quadratic in time (consider eqs 2 and 6). Fig. 14 shows the rate of change of CAM prediction from single epoch flows from Fig. 13, and a full range of constant acceleration flows. The two methods are seen to be in good agreement. However, there is no stability with respect to fitting the observations: either

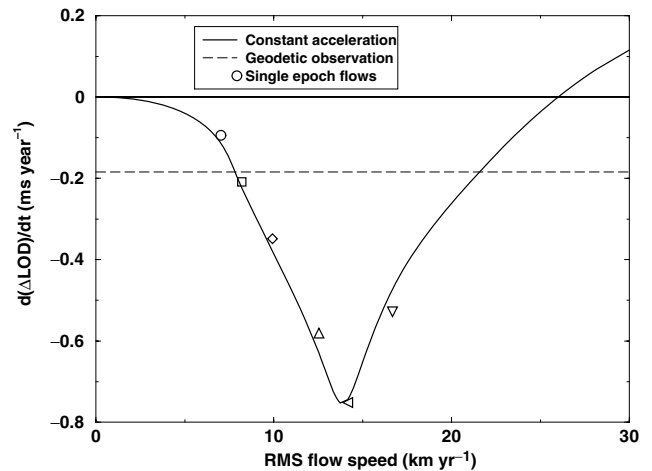


Figure 14. Rate of change of angular momentum for fits to single epoch flows, and constant acceleration flows, compared with geodetic prediction. Symbols represent gradient of best-fit line from corresponding set of solutions in Fig. 13.

flows of low- or high-strength match the observed ΔLOD , but intermediate flows produce a change that is four times too great. This is unexpected: calculations for the period 1900–1990 managed to reproduce the approximate structure of the change in LOD for a wide variety of flow complexities and *a priori* information (Holme & Whaler 1998).

What could be going wrong? The diffusional error parametrization from Fig. 6 is not the cause: minimizing solely the misfit to SV at the Earth's surface produces an even wider range of estimates for CAM rate of change. The solution to this problem may be revealed by the analysis of another time-dependent field model, developed while this paper was under review (Olsen *et al.* 2006). This new model has a more sophisticated treatment of external field sources, in particular allowing for direct determination of the magnetospheric ring current and how it varies with time, rather than parametrization in terms of the Dst index calculated from magnetic observatory measurements. The LOD prediction of that model shows uniform values of about -0.4 ms yr^{-1} for flow speeds between 10 and 20 km yr^{-1} . The magnitude of these values is still too high, but shows encouraging similarity over a range of flow magnitudes. As such, rejection of finer-scale flows as presented here due to arguments based on angular momentum calculation may be premature. It could be that in the CO2003 model, inadequately modelled external field led to large uncertainties in magnetic secular acceleration, and hence to the rate of change of angular momentum calculation. However, the greater impact of non-uniqueness on the fine-scale flows could also be significant. Consider flow around a mid-latitude closed contour of geostrophic degeneracy. The calculation of angular momentum assumes no variation in motion in the direction of the rotation axis: therefore, such a vortex is considered as a cylindrical rotation throughout the core. Such a motion has angular momentum in the direction of the rotation axis, and so contributes to the estimated CAM. Thus, uncertainty in flow around contours of the geostrophic degeneracy will directly influence the CAM prediction.

8 CONCLUSION

We have analysed the CO2003 model of magnetic secular variation calculated from data from magnetic satellites. The power spectrum of this model is 'blue' at the CMB: power increases with harmonic degree. While diffusion is likely to contribute to core SV , nevertheless the shape of the spectrum suggests that advection is likely to be an important process in generating SV to high harmonic degrees, and indeed, a simple physical argument suggests that diffusion may be relatively more important in flow modelling at low harmonic degree. As a result, it will be difficult to constrain diffusion in the core based upon the new models of secular variation.

Calculating flows with fine-scale features from this SV model is fraught with difficulties. In particular, the formal non-uniqueness plays a larger role than with large-scale flows, because now the flow has significant power at degrees which can produce flow along non-uniqueness contours. Nevertheless, we tentatively confirm previous claims of flow features, which might result from vortex motion in the inner core tangent cylinder. For the CO2003 model, the additional fine-scale flow detail seems to destabilize estimates of CAM, which is worrying; without a good comparison between CAM and observed ΔLOD , we have no independent control on whether the calculated flows are meaningful. However, more recent models calculated during revision of this paper suggest that with longer satellite data series, and in particular a better modelling of the time-varying

external field, fine-scale flows may also show coherent values for CAM estimates.

It seems clear that we require better methodology in dealing with both diffusion, and flow non-uniqueness. Such insights are most likely to come from the study of the output of numerical dynamo codes (e.g. Rau *et al.* 2000), which allow us to compare modelled flow with the true flow which generates their SV . This has been begun by Olson *et al.* (2002) to examine the influence of diffusion, and by Amit & Olson (2004) to explore for additional *a priori* information in terms of the vorticity of the flow, particularly useful in attempts to resolve vortical flow along contours of the geostrophic degeneracy. Extracting physical information from high-resolution SV is likely to be a long-term undertaking.

ACKNOWLEDGMENTS

RH thanks Andrew Jackson for useful discussions. Coerte Voorhies provided an extremely thorough and useful review. Flow plots were generated using GMT (Wessel & Smith 1998).

REFERENCES

- Amit, H. & Olson, P., 2004. Helical core flow from geomagnetic secular variation, *Phys. Earth planet. Int.*, **147**, 1–25.
- Backus, G.E., 1968. Kinematics of geomagnetic secular variation in a perfectly conducting core, *Phil. Trans. R. Soc. Lond., A*, **263**, 239–266.
- Backus, G.E. & Le Mouél, J.-L., 1986. The region on the core-mantle boundary where a geostrophic velocity field can be determined from frozen flux magnetic data, *Geophys. J. R. astr. Soc.*, **85**, 617–628.
- Benton, E.R. & Whaler, K.A., 1983. Rapid diffusion of the poloidal geomagnetic field through the weakly conducting mantle: a perturbation solution, *Geophys. J. R. astr. Soc.*, **75**, 77–100.
- Bloxham, J., 1988. The dynamical regime of fluid flow at the core surface, *Geophys. Res. Lett.*, **15**, 585–588.
- Bloxham, J., 1990. On the consequences of strong stable stratification at the top of the Earth's outer core, *Geophys. Res. Lett.*, **17**, 2081–2084.
- Bloxham, J. & Jackson, A., 1991. Fluid flow near the surface of the Earth's outer core, *Rev. Geophys.*, **29**, 97–120.
- Bloxham, J. & Jackson, A., 1992. Time-dependent mapping of the magnetic field at the core-mantle boundary, *J. geophys. Res.*, **97**, 19 537–19 563.
- Bondi, H. & Gold, T., 1950. On the generation of magnetism by fluid motion, *Mon. Not. R. Astron. Soc.*, **110**, 607–611.
- Braginsky, S.I., 1970. Torsional magnetohydrodynamic vibrations in the Earth's core and variations in day length, *Geomag. and Aeronomy (English translation)*, **10**, 1–8.
- Cain, J.C., Wang, Z., Kluth, C. & Schmitz, D.R., 1989a. Derivation of a geomagnetic model to $n = 63$, *Geophys. J.*, **97**, 431–441.
- Cain, J.C., Wang, Z., Schmitz, D.R. & Meyer, J., 1989b. The geomagnetic spectrum for 1980 and core-crustal separation, *Geophys. J.*, **97**, 443–447.
- De Santis, A., Barraclough, D.R. & Tozzi, R., 2003. Spatial and temporal spectra of the geomagnetic field and their scaling properties, *Phys. Earth planet. Int.*, **135**, 125–134.
- Eymin, C. & Hulot, G., 2005. On core surface flows inferred from magnetic satellite data, *Phys. Earth planet. Int.*, **152**, 200–220.
- Gubbins, D., 1982. Finding core motions from magnetic observations, *Phil. Trans. R. Soc. Lond., A*, **306**, 247–254.
- Gubbins, D., 1996. A formalism for the inversion of geomagnetic data for core motions with diffusion, *Phys. Earth planet. Int.*, **98**, 193–206.
- Gubbins, D. & Kelly, P., 1996. A difficulty with using the frozen flux hypothesis to find steady core motions, *Geophys. Res. Lett.*, **23**, 1825–1828.
- Gubbins, D. & Roberts, P.H., 1987. Magnetohydrodynamics of the Earth's core, in *Geomagnetism*, Vol. 2, chap. 1, ed. Jacobs, J.A., Academic, San Diego, Calif.

- Hills, R.G., 1979. Convection in the Earth's mantle due to viscous shear at the core-mantle interface and due to large-scale buoyancy, *PhD thesis*, New Mexico State University, Las Cruces.
- Holme, R., 1998. Electromagnetic core-mantle coupling I: explaining decadal variations in the Earth's length of day, *Geophys. J. Int.*, **132**, 167–180.
- Holme, R. & de Viron, O., 2005. Geomagnetic jerks and a high-resolution length-of-day profile for core studies, *Geophys. J. Int.*, **160**, 435–439.
- Holme, R. & Jackson, A., 1997. The cause and treatment of anisotropic errors in near-Earth geomagnetic data, *Phys. Earth planet. Int.*, **103**, 375–388.
- Holme, R. & Olsen, N., 2005. The spectrum of the magnetic secular variation, in *Earth Observation with CHAMP—results from Three Years in Orbit*, pp. 329–334, Springer Verlag, Berlin.
- Holme, R. & Whaler, K.A., 1998. Issues in core-flow modelling and core angular momentum, *EOS Trans. Am. geophys. Un.*, **79**, F231.
- Holme, R. & Whaler, K.A., 2001. Steady core flow in an azimuthally drifting reference frame, *Geophys. J. Int.*, **145**, 560–569.
- Hulot, G. & Le Mouél, J.L., 1994. A statistical approach to the Earth's main magnetic field, *Phys. Earth planet. Int.*, **82**, 167–183.
- Hulot, G., Eymin, C., Langlais, B., Manda, M. & Olsen, N., 2002. Small-scale structure of the geodynamo inferred from Oersted and MAGSAT satellite data, *Nature*, **416**, 620–623.
- Jackson, A., 1995. An approach to estimation problems containing uncertain parameters, *Phys. Earth planet. Int.*, **90**, 145–156.
- Jackson, A., 1997. Time dependency of geostrophic core surface motions, *Phys. Earth planet. Int.*, **103**, 293–311.
- Jackson, A. & Hide, R., 1996. Invariants in toroidal and tangentially geostrophic frozen-flux velocity fields, *Geophys. J. Int.*, **125**, 925–927.
- Jackson, A., Bloxham, J. & Gubbins, D., 1993. Time-dependent flow at the core surface and conservation of angular momentum in the coupled core-mantle system, in *Dynamics of the Earth's deep interior and Earth rotation*, pp. 97–107, eds Le Mouél, J.-L., Smylie, D.E. & Herring, T., AGU/IUGG, Washington, DC.
- Jault, D., Gire, C. & Le Mouél, J.L., 1988. Westward drift, core motions and exchanges of angular momentum between core and mantle, *Nature*, **333**, 353–356.
- Langel, R.A. & Estes, R.H., 1982. A geomagnetic field spectrum, *Geophys. Res. Lett.*, **9**, 250–253.
- Le Mouél, J.-L., 1984. Outer core geostrophic flow and secular variation of Earth's magnetic field, *Nature*, **311**, 734–735.
- Love, J.J., 1999. A critique of frozen-flux inverse modelling of a nearly steady geodynamo, *Geophys. J. Int.*, **138**, 353–365.
- Loves, F.J., 1974. Spatial power spectrum of the main geomagnetic field, and extrapolation to the core, *Geophys. J. R. astr. Soc.*, **36**, 717–730.
- Loves, F.J. & Olsen, N., 2004. A more realistic estimate of the variances and systematic errors in spherical harmonic geomagnetic field models, *Geophys. J. Int.*, **157**, 1027–1044.
- Mauersberger, P., 1956. Das Mittel der Energiedichte des geomagnetischen Hauptfeldes an der Erdoberfläche und seine säkulare Änderung, *Gerlands Beitr. Geophys.*, **65**, 207–215.
- Maus, S., Rother, M., Holme, R., Lühr, H., Olsen, N. & Haak, V., 2002. First scalar magnetic anomaly map from CHAMP satellite data indicates weak lithospheric field, *Geophys. Res. Lett.*, **29**, 10.1029/2001GL013685.
- McLeod, M.G., 1985. Statistical theory of the geomagnetic field and its secular variation, *EOS, Trans. Am. geophys. Un.*, **66**(46), 878.
- McLeod, M.G., 1996. Spatial and temporal power spectra of the geomagnetic field, *J. geophys. Res.*, **101**, 2745–2763.
- Neubert, T. et al., 2001. Ørsted satellite captures high-precision geomagnetic field data, *EOS, Trans. Am. geophys. Un.*, **82**, 81–88.
- Olsen, N., 2002. A model of the geomagnetic field and its secular variation for epoch 2000 estimated from Ørsted data, *Geophys. J. Int.*, **149**, 454–462.
- Olsen, N. et al., 2000. Ørsted initial field model, *Geophys. Res. Lett.*, **27**, 3607–3610.
- Olsen, N., Lühr, H., Sabaka, T.J., Manda, M., Rother, M., Tøffner-Clausen, L. & Choi, S., 2006. CHAOS - a model of Earth's magnetic field derived from CHAMP, Ørsted and SAC-C magnetic satellite data, *Geophys. J. Int.*, **166**, 67–75.
- Olson, P. & Aurnou, J., 1999. A polar vortex in the earth's core, *Nature*, **402**, 170–173.
- Olson, P., Christensen, U. & Glatzmaier, G.A., 1999. Numerical modeling of the geodynamo: Mechanisms of field generation and equilibration, *J. geophys. Res.*, **104**, 10 383–10 404.
- Olson, P., Sumita, I. & Aurnou, J., 2002. Diffusive magnetic images of upwelling patterns in the core, *J. geophys. Res.*, **107**, 2348.
- Olver, F.J., 1960. *Bessel Functions Part III: Zeros and Associated Values*, Vol. 7 of Royal Society Mathematical Tables, CUP, Cambridge.
- Rau, S., Christensen, U., Jackson, A. & Wicht, J., 2000. Core flow inversion tested with numerical dynamo models, *Geophys. J. Int.*, **141**, 485–497.
- Reigber, C., Lühr, H. & Schwintzer, P., 2002. CHAMP mission status, *Adv. Space Res.*, **30**, 129–134.
- Roberts, P.H., 1987. Origin of the main field: dynamics, in *Geomagnetism*, Vol. 2, chap. 3, ed. Jacobs, J.A., Academic, London.
- Sabaka, T.J., Olsen, N. & Langel, R.A., 2004. Extending comprehensive models of the Earth's magnetic field with ørsted and CHAMP data, *Geophys. J. Int.*, **159**, 521–547.
- Stephenson, F.R. & Morrison, L.V., 1995. Long-term fluctuations in the Earth's rotation—700 B.C. to A.D. 1990, *Phil. Trans. R. Soc. Lond., A*, **351**, 165–202.
- Tyler, R.H., Maus, S. & Lühr, H., 2003. Satellite observations of magnetic fields due to ocean tidal flow, *Science*, **299**, 239–241.
- Vestine, E.H., 1953. On variations of the geomagnetic field, fluid motions, and the rate of Earth's rotation, *J. geophys. Res.*, **58**, 127, 145.
- Voorhies, C.V., 1993. Geomagnetic estimates of steady surficial core flow and flux diffusion: unexpected geodynamo experiments, in *Dynamics of the Earth's deep interior and Earth rotation*, pp. 113–125, eds Le Mouél, J.-L., Smylie, D.E. & Herring, T., AGU/IUGG.
- Voorhies, C.V., 1995. Time-varying fluid-flow at the top of Earth's core derived from definitive geomagnetic reference field models, *J. geophys. Res.*, **100**, 10 029–10 039.
- Voorhies, C.V., 2004. Narrow scale flow and a weak field by the top of Earth's core: evidence from Ørsted, MAGSAT and secular variation, *J. geophys. Res.*, **109**, B03106, doi:10.1029/2003JB002833.
- Voorhies, C.V. & Backus, G.E., 1985. Steady flows at the top of the core from geomagnetic-field models—the steady motions theorem, *Geophys. Astrophys. Fluid Dyn.*, **32**, 163–173.
- Voorhies, C.V. & Benton, E.R., 1982. Pole-strength of the Earth from MAGSAT and magnetic determination of the core radius, *Geophys. Res. Lett.*, **9**, 258–261.
- Voorhies, C.V., Sabaka, T.J. & Purucker, M., 2002. On magnetic spectra of Earth and Mars, *J. geophys. Res.*, **107**, doi:10.1029/2001JE001534.
- Wessel, P. & Smith, W.H.F., 1998. New, improved version of the generic mapping tools released, *EOS, Trans. Am. geophys. Un.*, **79**, 579.
- Whaler, K.A., 1980. Does the whole of the Earth's core convect?, *Nature*, **287**, 528–530.
- Whaler, K.A., 1986. Geomagnetic evidence for fluid upwelling at the core-mantle boundary, *Geophys. J. R. astr. Soc.*, **86**, 563–588.
- Whaler, K.A. & Davis, R.G., 1997. Probing the Earth's core with geomagnetism, in *Earth's Deep Interior*, pp. 114–166, ed. Crossley, D.J., Gordon and Breach, Amsterdam.